Analysis of Singularities and Edge Detection using the Shearlet Transform

Glenn Easley [(1)], Kanghui Guo [(2)], and Demetrio Labate [(3)]

(1) System Planning Corporation 1000 Wilson Boulevard, Arlington, VA 22209, USA.
(2) Missouri State University, Springfield, MO 65804, USA.
(3) University of Houston, 651 Phillip G Hoffman, Houston, TX 77204-3008, USA.
geasley@sysplan.com, KanghuiGuo@MissouriState.edu, dlabate@math.uh.edu

Abstract:

The continuous curvelet and shearlet transforms have recently been shown to be much more effective than the traditional wavelet transform in dealing with the set of discontinuities of functions and distributions. In particular, the continuous shearlet transform has the ability to provide a very precise geometrical characterization of general discontinuity curves occurring in images. In this paper, we show that these properties are useful to design improved algorithms for the analysis and detection of edges.

1. Introduction

One of the most useful properties of the wavelet transform is its ability to deal very efficiently with the discontinuities of functions and distributions. Consider, for example, a function f on $\mathbb{R}^2$ which is smooth except for a discontinuity at $x_0 \in \mathbb{R}^2$, and let $\mathcal{W}_\psi f(a,t)$ be the *continuous wavelet transform* of f. This is defined as the mapping

$$\mathcal{W}_\psi f(a,t) = a^{-1} \int_{\mathbb{R}^2} f(x)\, \psi\left(a^{-1}(x-t)\right)\, dx,$$

where $a > 0, t \in \mathbb{R}^2$ and $\psi \in L^2(\mathbb{R}^2)$ is an appropriate well-localized function. Then $\mathcal{W}_\psi f(a,t)$ decays rapidly as $a \to 0$ everywhere, unless t is near x_0 [5]. Hence, the wavelet transform is able to signal the location of the singularity of f through its asymptotic decay at fine scales. It was recently shown that certain "directional" extensions of the wavelet transform have the ability to provide a much finer description of the set of singularities of a function. Namely, the recently introduced curvelet and shearlet transforms are able to identify not only the location of singularities of a function, but also the orientation of discontinuity curves. In particular, using the continuous shearlet transform, one can precisely characterize the geometrical information of general discontinuity curves, including discontinuity curves which contain irregularities such as corner and junction points.

In this paper, we show that one can take advantage of the properties of the shearlet transform to design improved algorithms for the analysis and detection of edges in images. Indeed, multiscale techniques based on wavelets have a history of successful applications in the study of edges. With respect to traditional wavelets, the shearlet framework has the ability to capture directly the information about edge orientation and this is useful to improve the robustness of edge detection algorithms in the presence of noise.

The paper is organized as follows. In Section 2. we recall the definition of the shearlet transform and its main results concerning the analysis of edges. In Section 3. we present some representative numerical experiments of edge detection, comparing the shearlet approach against wavelets and other standard edge detection techniques.

2. The Shearlet Transform

For $a > 0$ $s \in \mathbb{R}$ and $t \in \mathbb{R}^2$, let M_{as} be the matrices

$$M_{as} = \begin{pmatrix} a & -\sqrt{a}s \\ 0 & \sqrt{a} \end{pmatrix}$$

and, corresponding to those, let $\psi_{ast}(x) = |\det M_{as}|^{-\frac{1}{2}} \psi(M_{as}^{-1}(x-t))$, where $\psi \in L^2(\mathbb{R}^2)$. It is useful to notice that $M_{as} = B_s\, A_a$, where $A_a = \begin{pmatrix} a & 0 \\ 0 & \sqrt{a} \end{pmatrix}$ and $B_s = \begin{pmatrix} 1 & -s \\ 0 & 1 \end{pmatrix}$. Hence to each matrix M_{as} are associated two distinct actions: an *anisotropic* dilation produced by the matrix A_a and a *shearing* produced by the non-expansive matrix B_s.

For $f \in L^2(\mathbb{R}^2)$, the *continuous shearlet transform* is defined as the mapping

$$f \to \mathcal{SH}_\psi f(a,s,t) = \langle f, \psi_{ast} \rangle,\ a > 0, s \in \mathbb{R}, t \in \mathbb{R}^2.$$

The generating function ψ is chosen to be a well localized function satisfying appropriate admissibility conditions [7, 4], so that each $f \in L^2(\mathbb{R}^2)$ satisfies the generalized Calderòn reproducing formula:

$$f = \int_{\mathbb{R}^2} \int_{-\infty}^{\infty} \int_0^{\infty} \langle f, \psi_{ast} \rangle\, \psi_{ast}\, \frac{da}{a^3}\, ds\, dt.$$

The significance of the shearlet representation is that any function f is broken up with respect to well-localized analyzing elements defined not only at various scales and locations, as in the traditional multiscale approach, but also at various orientations associated with the shearing parameter s. Figure 1 shows the frequency support of the shearlet analyzing functions $\hat{\psi}_{ast}$ for some values of s and a. Thanks to this directional multiscale decomposition, the continuous shearlet transform is able to precisely capture the geometry of edges through its asymptotic decay at fine

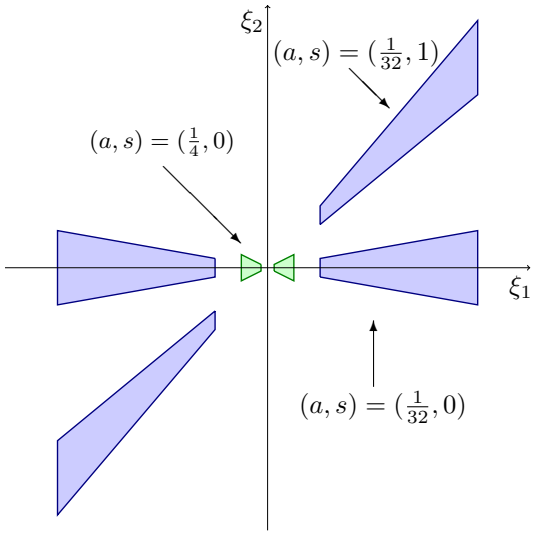

Figure 1: Frequency support of same representative shearlet analyzing functions $\hat{\psi}_{ast}$.

scales ($a \to 0$). To precisely describe these properties, let us introduce the following model of images.
Let $\Omega = [0,1]^2$ and consider the partition $\Omega = \bigcup_{n=1}^{L} \Omega_n \cup \Gamma$, where:

1. each "object" Ω_n, for $n = 1, \ldots, L$, is a connected open set;
2. the set of edges of Ω is given by $\Gamma = \bigcup_{n=1}^{L} \partial_\Omega \Omega_n$, where each boundary $\partial_\Omega \Omega_n$ is a piecewise smooth curve of finite length.

Hence, we consider the space of images $u \in I(\Omega)$ of the form

$$u(x) = \sum_{n=1}^{L} u_n(x)\, \chi_{\Omega_n}(x) \text{ for } x \in \Omega \backslash \Gamma$$

where, for each $n = 1, \ldots, L$, $u_n \in C_0^1(\Omega)$ has bounded partial derivatives, and the sets Ω_n are pairwise disjoint in measure. We have the following result, which is a significant refinement with respect to the simple detection of singularities obtained using traditional wavelets.

Theorem 2.1. *Let $f \in I(\Omega)$.*

(i) If $t \notin \Gamma$, then, for each $N \in \mathbb{N}$

$$\lim_{a \to 0^+} a^{-N}\, \mathcal{SH}_\psi f(a,s,t) = 0.$$

(ii) If $t \in \Gamma$ is a regular point and s does not correspond to the normal direction of Γ at t then

$$\lim_{a \to 0^+} a^{-N}\, \mathcal{SH}_\psi B(a,s,t) = 0, \quad \text{for all } N > 0;$$

otherwise, if $s = s_0$ corresponds to the normal direction of Γ at t then

$$0 < \lim_{a \to 0^+} a^{-\frac{3}{4}} \left| \mathcal{SH}_\psi B(a, s_0, t) \right| < \infty.$$

(iii) If $t \in \Gamma$ is a corner point and s does not correspond to any of the normal directions of Γ at t, then

$$\lim_{a \to 0^+} a^{-\frac{9}{4}} \left| \mathcal{SH}_\psi B(a,s,t) \right| < \infty;$$

otherwise, if $s = s_0$ corresponds to one of the normal directions of Γ at t then

$$0 < \lim_{a \to 0^+} a^{-\frac{3}{4}} \left| \mathcal{SH}_\psi B(a, s_0, t) \right| < \infty.$$

Thus, the continuous shearlet transform has rapid asymptotic decay, as $a \to 0$, everywhere except for locations t on the edges and orientations s which are normal to the edges. We refer to [7, 4, 3] for additional detail, including a more precise description of the behavior at the corner points. We also refer to [1] for some similar (even if more restricted) results based on the curvelet transform.

2.1 Lipschitz regularity

The notion of Lipschitz regularity is a method to quantitatively describe the local regularity of functions and distributions.
Given $\alpha \geq 0$, a function f is Lipschitz α at $x_0 \in \mathbb{R}^2$ if there exists a positive constant K and a polynomial p_{x_0} of degree $m = \lfloor \alpha \rfloor$ such that, for all x in a neighborhood of x_0:

$$|f(x) - p_{x_0}(x)| \leq K\, |x - x_0|^\alpha . \tag{1}$$

A function f is uniformly Lipschitz α over an open set $\Omega \subset \mathbb{R}^2$ if there exists a constant $K > 0$, independent of x_0, such that the above inequality holds for all $x_0 \in \Omega$.
If f is uniformly Lipschitz $\alpha > m$ in a neighborhood of x_0, then f is necessarily m times differentiable at x_0. Also notice that if $0 \leq \alpha < 1$, then $p_{x_0} = f(x_0)$ and condition (1) becomes

$$|f(x) - f(x_0)| \leq K\, |x - x_0|^\alpha .$$

If f is Lipschitz α with $\alpha < 1$ at x_0, then f is not differentiable at x_0. The closer the Lipschitz exponent is to 0, the more "singular" the function is. If f is bounded but discontinuous at x_0, then it is Lipschitz 0 at x_0, indicating the presence of an edge.
Also recall that if $f(x)$ is Lipschitz α, then its primitive $g(x)$ is Lipschitz α + 1 (the converse however is not true; that is, if a function is Lipschitz α at x_0, then its derivative need not be Lipschitz α - 1 at the same point). This observation explains the following definition which extends the concept of Lipschitz regularity to distributions.
Let α be a real number. A tempered distribution f is uniformly Lipschitz α on $\Omega \subset \mathbb{R}^2$ if its primitive is uniformly Lipschitz $\alpha + 1$ on $\Omega \subset \mathbb{R}^2$.
It follows that a distribution may have a negative Lipschitz exponent. For example, one can show that if f is a Dirac delta distribution centered at x_0, then f is Lipschitz -1 at x_0. We refer to [8] and to the references indicated there for more details.
The function ψ satisfies the property that for each $n \in \mathbb{N}$, there exists a constant $c_n > 0$ such that

$$|\psi(x)| \leq c_n (1 + |x|)^{-n}$$

for all $x \in \mathbb{R}^2$ (for details, see [4], p. 26). As a consequence, we obtain $\|\psi\|_1 = \int_{\mathbb{R}^2} |\psi(x)|\, dx < \infty$, and $\int_{\mathbb{R}^2} |\psi(x)||x|^\alpha\, dx < \infty$.
The following result (whose proof is reported in the appendix) is an adaptation of a similar theorem about the

continuous wavelet transform due to Jaffard [6]. If we assume ψ has n vanishing moments, i.e. $\int t^k \psi(t)\, dt = 0$ for all $k = 0, \ldots, n-1$, we would need to add the condition $\alpha \leq n$. However, the general construction of ψ implies that ψ has an infinite number of vanishing moments. Thus this assumption is unnecessary.

Theorem 2.2. *If $f \in L^2(\mathbb{R}^2)$ is Lipschitz $\alpha > 0$ at t_0, then there exists a constant $C > 0$ such that, for all $a < 1$,*

$$|\mathcal{SH}_\psi f(a, s, t)| \leq C\, a^{\frac{1}{2}(\alpha+\frac{3}{2})} \left(1 + \left|a^{-\frac{1}{2}}(t - t_0)\right|\right).$$

The theorem can be extended to the case where f is a distribution. In addition, the estimation of the decay of the shearlet transform of the Dirac delta and other distributions was computed in [7]. These results show that, for locations t corresponding to delta-type singularities, the shearlet transform has a very different behavior from edge points. In fact, the amplitude of $|\mathcal{SH}_\psi f(a, s, t_0)|$ grows like $O(a^{-\frac{1}{4}})$ as $a \to 0$. Similarly, for spike singularities, one can show that the amplitude of the shearlet transform increases at fine scales. This shows that classification of points by their Lipschitz regularity is important as it can be used to distinguish true edge points from points corresponding to noise. This principle was already exploited, for example, in [8].

3. Shearlet-based Edge Detection

Taking advantage of the theoretical observations reported above, a discrete version of the shearlet transform was developed and applied to the purpose of locating and identifying edges in images. Because of space limitations, we will limit ourselves to presenting a few numerical demonstrations. A detailed account of the discrete shearlet transform and shearlet-based edge detection algorithms is found in [2, 10].

Figures 2 and 3 compare a shearlet-based edge detection routine against a wavelet-based routine using a consistent set of predetermined default parameters. For a base-line comparison against standard routines, we also used the Sobel and Prewitt methods using their default parameters. The results highlight the superior performance of the shearlet-based method. To assess the performance of the edge detector, we have given the value of the Pratt's Figure of Merit (FOM), which is a fidelity measure ranging from 0 to 1, with 1 indicating a perfect edge detector [9].

Acknowledgments DL acknowledges partial support from NSF DMS 0604561 and DMS (Career) 0746778.

4. Appendix: Proof of Theorem 2.2.

Proof of Theorem 2.2. Since f is Lipschitz α at t_0, there is a polynomial $p_{t_0}(x)$ and a constant $K > 0$ such that

$$|f(x) - p_{t_0}(x)| \leq K\, |x - t_0|^\alpha.$$

Since $\mathcal{SH}_\psi p_{t_0}(a, s, t) = 0$, then

$$\begin{aligned}
& |\mathcal{SH}_\psi f(a, s, t)| \\
\leq\ & a^{-3/4} \int_{\mathbb{R}^2} |\psi(A_a^{-1} B_s^{-1}(x - t))|\, |f(x) - p_{t_0}(x)|\, dx \\
\leq\ & K\, a^{-3/4} \int_{\mathbb{R}^2} |\psi(A_a^{-1} B_s^{-1}(x - t))|\, |x - t_0|^\alpha\, dx \\
=\ & K\, a^{3/4} \int_{\mathbb{R}^2} |\psi(y)|\, |t + B_s A_a y - t_0|^\alpha\, dy \\
\leq\ & K\, 2^\alpha\, a^{3/4} \left(\|B_s\|^\alpha\, \|A_a\|^\alpha \int_{\mathbb{R}^2} |\psi(y)|\, |y|^\alpha\, dy \right. \\
& \left. + \int_{\mathbb{R}^2} |\psi(y)|\, |t - t_0|^\alpha\, dy \right) \\
\leq\ & K\, 2^\alpha\, a^{3/4} \left(C(s)^\alpha\, a^{\alpha/2} \int_{\mathbb{R}^2} |\psi(y)|\, |y|^\alpha\, dy \right. \\
& \left. + |t - t_0|^\alpha \int_{\mathbb{R}^2} |\psi(y)|\, dy \right) \\
\leq\ & C\, a^{\frac{1}{2}(\alpha+\frac{3}{2})} \left(1 + |a^{-1/2}(t - t_0)|^\alpha\right).
\end{aligned}$$

Here we have used the fact that $\|A_a\| = a^{1/2}$, i.e. the largest eigenvalue of the matrix A_a. Similarly $\|B_s\|$ is the largest eigenvalue of the matrix B_s, which is 1.

References:

[1] E. J. Candès and D. L. Donoho, "Continuous curvelet transform: I. Resolution of the wavefront set", *Appl. Comput. Harmon. Anal.*, Vol. 19, pp. 162–197, 2005. 162–197.

[2] G. Easley, D. Labate, and W-Q. Lim "Sparse Directional Image Representations using the Discrete Shearlet Transform", *Appl. Comput. Harmon. Anal.* Vol. 25, pp. 25–46, 2008.

[3] K. Guo and D. Labate, "Characterization and analysis of edges using the Continuous Shearlet Transform", preprint, 2008

[4] K. Guo, D. Labate and W. Lim, "Edge analysis and identification using the continuous shearlet transform", to appear in *Appl. Comput. Harmon. Anal.*.

[5] M. Holschneider, *Wavelets. Analysis tool*, Oxford University Press, Oxford, 1995.

[6] S. Jaffard "Pointwise smoothness, two-localization and wavelet coefficients", *Publicacions Mathematique*, Vol. 35, pp. 155–168, 1991.

[7] G. Kutyniok and D. Labate, "Resolution of the Wavefront Set using Continuous Shearlets", *Trans. Am. Math. Soc.*, Vol. 361 pp. 2719-2754, 2009.

[8] S. Mallat and W. L. Hwang, Singularity detection and processing with wavelets, *IEEE Trans. Inf. Theory*, vol. 38, no. 2, 617-643, Mar. 1992.

[9] W.K. Pratt, *Digital Image Processing*, Wiley Interscience Publications, 1978.

[10] S. Yi, D. Labate, G. R. Easley, and H. Krim, "A Shearlet Approach to Edge Analysis and Detection", to appear in IEEE Trans. Image processing, 2008.

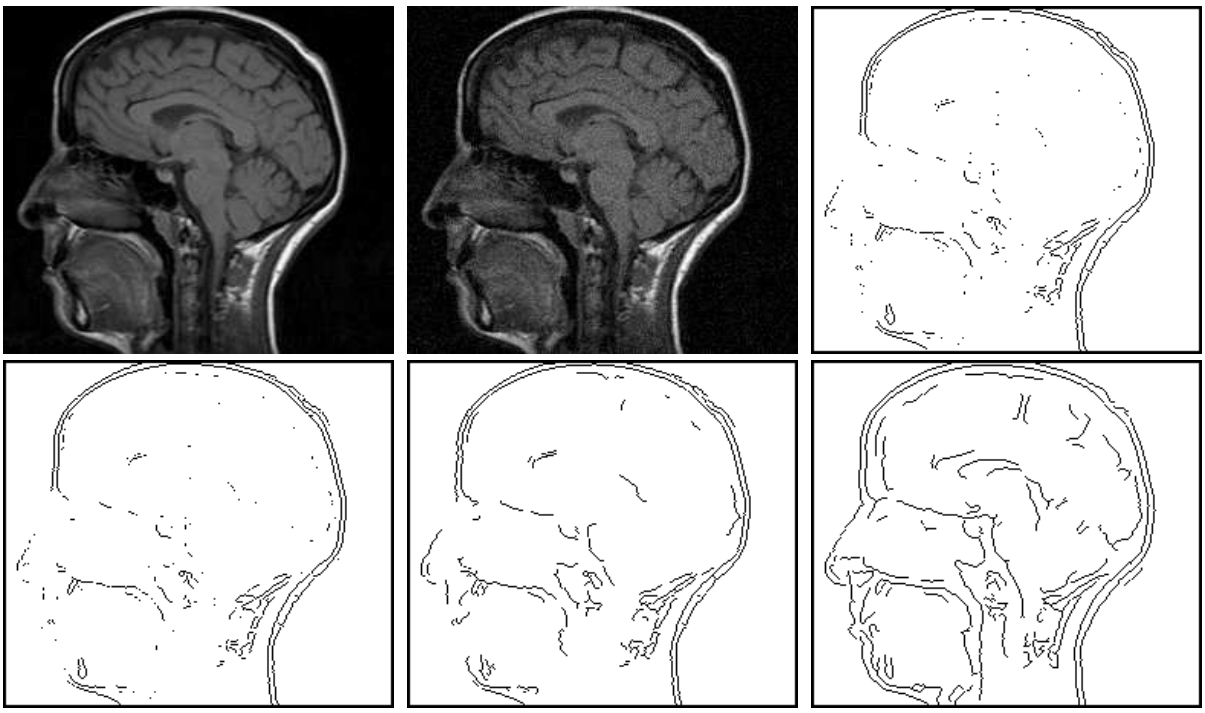

Figure 2: Results of edge detection methods. From top left, clockwise: Original image, noisy image (PSNR=28.10 dB), Sobel result (FOM=0.24), shearlet result (FOM=0.44), wavelet result (FOM=0.29), and Prewitt result (FOM=0.23).

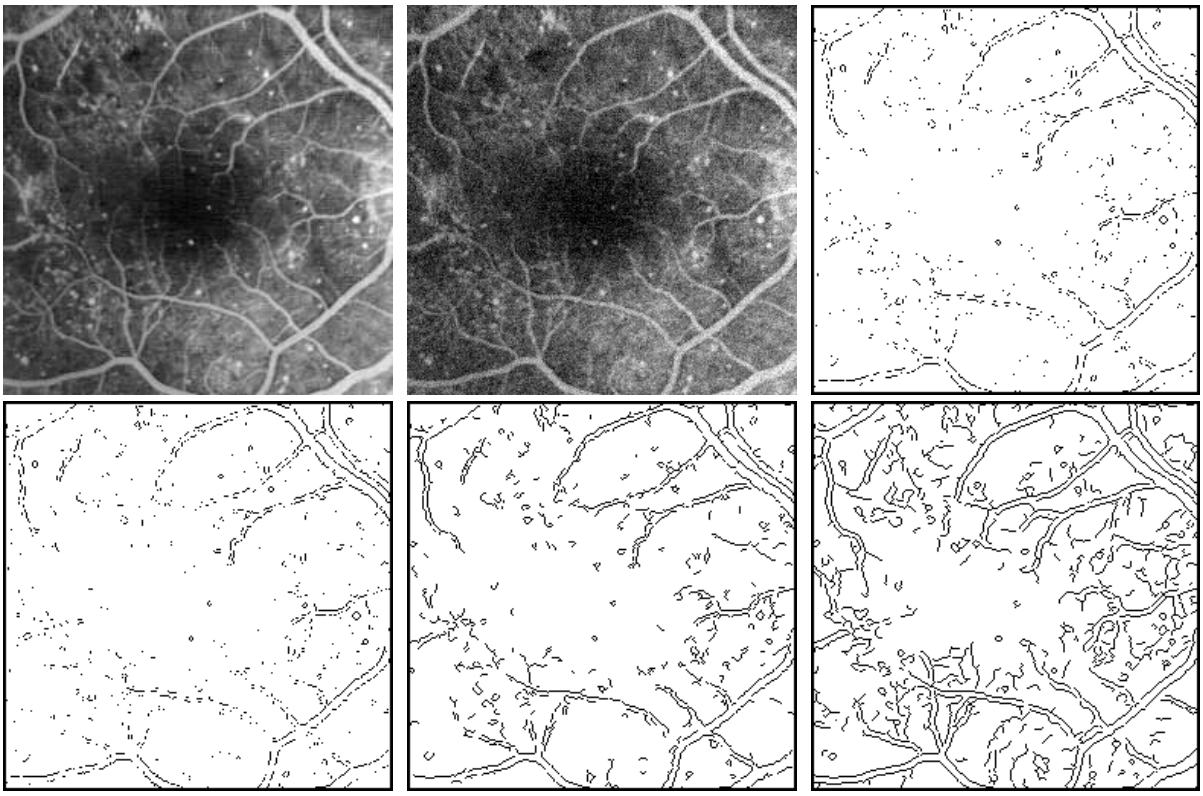

Figure 3: Results of edge detection methods. From top left, clockwise: Original image, noisy image (PSNR=24.58 dB), Sobel result (FOM=0.15), shearlet result (FOM=0.45), wavelet result (FOM=0.27), and Prewitt result (FOM=0.15).